

TCFE6: TCS Steel and Fe-alloys Database

Thermo-Calc Software is pleased to announce the release of TCFE6, a thermodynamic database for different kinds of steels and Fe-based alloys (stainless steels, high-speed steels, tool steels, HSLA steels, cast iron, corrosion-resistant high strength steels and more) for use with the Thermo-Calc and DICTRA software packages. In order to increase the predictive capability of the database, several significant re-assessments have been performed by Thermo-Calc Software AB and incorporated in the new release. The element Ca has been added and the alloying ranges for the elements C, Co, Cu, N, Ti and V have been extended. In version 4 (TCFE4), all necessary volume data (including molar volume and thermal expansion) for various alloy phases were incorporated; such volume data has been updated for all phases in this new release. However, the molar volume data incorporated has no pressure dependence.

Some of the major improvements to the TCFE6 database include improved thermodynamic descriptions for the following ternary and quaternary systems (with many sub-systems also re-assessed):

Al-Co-Si	Al-Cr-B	Al-Fe-C
Al-Fe-Ni	Al-Fe-Mn	C-Co-W
Cr-Cu-Ni	Cr-Mn-O	Cr-Mo-C
Cr-V-N	Fe-Al-C	Fe-Al-Cr
Fe-Al-Mn	Fe-Al-Ni	Fe-B-C
Fe-B-Co	Fe-B-Cr	Fe-B-Mn
Fe-B-Mo	Fe-B-N	Fe-B-Nb
Fe-B-Ni	Fe-B-Si	Fe-B-V
Fe-B-W	Fe-B-Ti	Fe-Co-V
Fe-Cr-Mo	Fe-Cr-Ni	Fe-Cr-W
Fe-Cu-V	Fe-Cu-S	Fe-Mn-C
Fe-Mn-O	Fe-Mo-C	Fe-Mo-W
Fe-Nb-C	Fe-Ni-C	Fe-Si-C
Fe-Ti-C	Fe-Ti-N	Mn-Ni-O
Mo-V-C	Mo-V-N	Nb-V-N
Al-Ca-Mg-O	Al-Ca-Si-O	C-Co-Nb-W
C-Co-V-W	Cr-V-W-C	Fe-Al-Cr-Ni
Fe-Ca-Mg-O	Fe-Ca-Mg-S	Fe-Co-Mo-C
Fe-Co-Mo-Si	Fe-Cr-Mo-N	Fe-Cr-Nb-C

Fe-Cr-Ni-O	Fe-Cr-Mn-O	Fe-Cr-V-C
Fe-Cr-V-N	Fe-Cr-W-C	Fe-Cu-Mn-S
Fe-Mn-Ni-O	Fe-Mo-Nb-C	Fe-Mo-Si-C
Fe-Mo-V-N	Fe-Nb-Si-C	Fe-Nb-V-C
Fe-Nb-W-C	Fe-V-W-C	Fe-W-Si-C
Nb-V-C-N	Nb-Ti-C-N	V-Ti-C-N

The SIGMA phase is described with a new model in TCFE6 and new phases such as KAPPA, Z_PHASE and DIGENITE, for example, have been added. Several elements; Al, B, Ca, Co, Cu, Mg, Nb, Ni, Si, V and Ti are modelled to dissolve in more phases such as LIQUID, FCC_A1, BCC_A2, LAVES_PHASE, different carbides, nitrides, sulphides and oxides. Major revisions regarding the solubility of Boron in LIQUID, FCC_A1, BCC_A2, HCP_A3, CEMENTITE, M23C6, M7C3, BN_HP4, CR2B_ORTH and M2B_TETR have been made, and in TCFE6 Boron is treated as an interstitial element.

In the TCFE6 database Al and Si have been implemented into the CEMENTITE phase. This is necessary to be able to calculate paraequilibrium between e.g. BCC_A2 and CEMENTITE for alloys containing Al and Si[1]. The CEMENTITE phase is described with two sublattices with the ratio 3:1, with the following constituents; (Al, Co, Cr, Fe, Mn, Mo, Nb, Ni, Si, V, W)₃(B, C, N)₁.

Ni and Si have been added to the LAVES_PHASE_C14, which is modelled with two sublattices with the ratio 2:1. The Si solubility in the laves phase can be relatively high as has been shown by Zhao et al.[2]. The solubility of many other elements has been previously included in the laves phase and with TCFE6, the description for the whole laves phase takes into account the elements Al, Co, Cr, Cu, Fe, Mg, Mn, Mo, Nb, Ni, Si, Ti and W. This new description has improved the accuracy of the predictions compared to experimental information[3-5].

Improvements in the Fe-Co-Cr-Mo-Nb-V-W-Ti-N-C system regarding the carbonitrides (M(C,N)), M7C3, M2C, M6C and M23C6 descriptions have been implemented.

The TCFE6 database contains an extensive GAS mixture phase (Ar and different species in the C-H-N-O-S system) for the main purpose of considering oxygen/nitrogen-gas controls in steel-making processes, and different gas atmospheres under e.g. heat treatments.

A new thermodynamic description of the Fe-C-Cr-Mn-Ni-O system[6-11] has been implemented. The present description of the SPINEL, HALITE and CORUNDUM phases and more, for the Fe-Al-Ca-Cr-Mg-Mn-Ni-Si-Ti-C-O system, in TCFE6 allows for accurate predictions in different fields, e.g. oxide scale formation on various steels[12-16]. In Figure 1 the oxide scale formed on a steel is predicted and the agreement to experimental information[12] is very good. One can see that below the outer scale (rich in corundum) a Fe-Mn spinel is formed and closest to the substrate a layer with halite and a Cr-Mn rich spinel, which also is verified in the work by Douglas et al.[12].

A new model for the spinel and corundum phases has been implemented which makes it possible to simulate diffusion inside these phases using the DICTRA software (also possible for other oxides such as halite) provided suitable mobility data are available.

TCFE6 contains molar volume data for all phases in the database (this was introduced first in TCFE4), which allows for the calculation of volume fraction of phases, as well as density and thermal expansivity using Thermo-Calc. Validation of predicted densities in different alloys are shown in Figure 7 and in Figure 8 the relative length change in a commercial steel is shown.

Validation of the TCFE6 database against experimental data shows that the new update is more accurate for predictions of:

- Tool steels and high-speed steels, especially in predicting correct phases and phase compositions. Figure 3 demonstrates the latter for a number of different tool steels and high-speed steels.
- HSLA steels, especially in predicting correct phases and phase compositions in all possible precipitates, see Figure 4 and Table 1.
- Solidification of cast irons and general steels. Inclusions containing complex oxides and sulphides, see Figure 5.
- Stainless steels, tool steels, high-speed steels and other Fe-based alloys with high concentrations of N.
- The relative stability between the austenite and ferrite phases in Al and Cu-rich alloys.
- The relative stability between the austenite and ferrite phases in alloys containing Al, Cr, Mn and Ni.
- Sulphides, oxides, borides and phosphides. Figure 1 and 2 shows calculation of oxide scale formation on a steel and a Fe-Cr-C alloy.
- Carbides, nitrides, carbonitrides and intermetallic phases such as sigma and laves phase.
- Liquidus and solidus temperatures. In addition, the accuracy to predict the correct primary phase to form from the liquid has increased. In Figure 6 measured liquidus temperatures are compared with calculated liquidus temperatures for various steels.

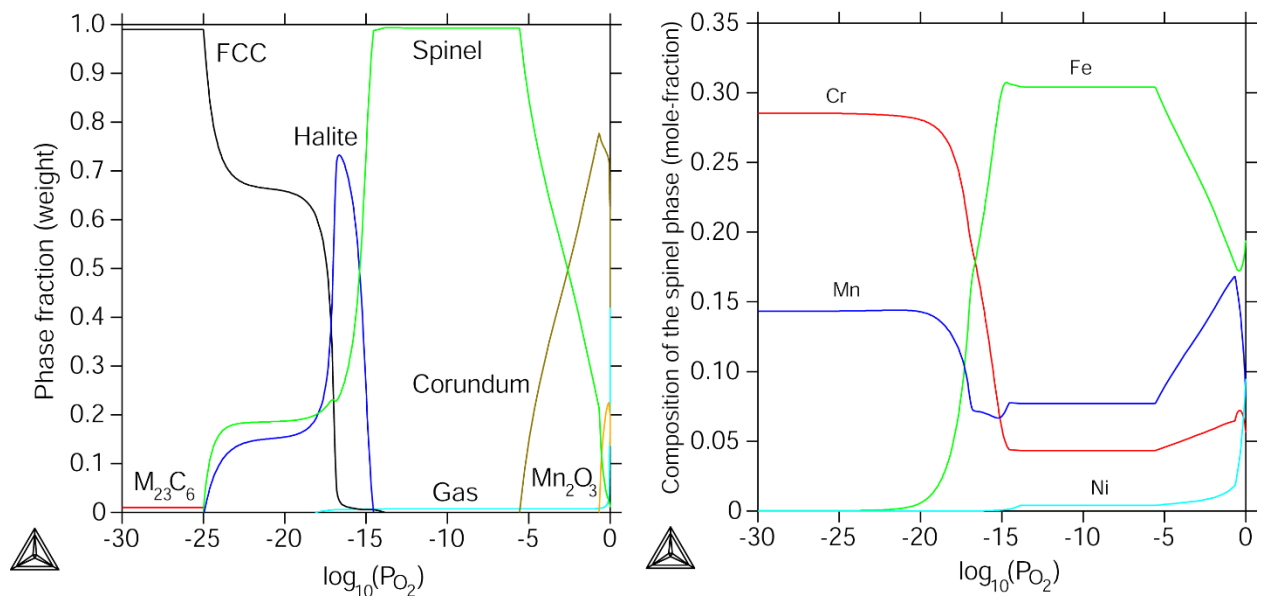


Figure 1. a) Oxidation of a steel (17.8 wt.% Mn, 9.5 Cr, 1.0 Ni and 0.27 C) at 900 °C. (b) Calculated composition of the spinel phase in the oxide scale at 900 °C.

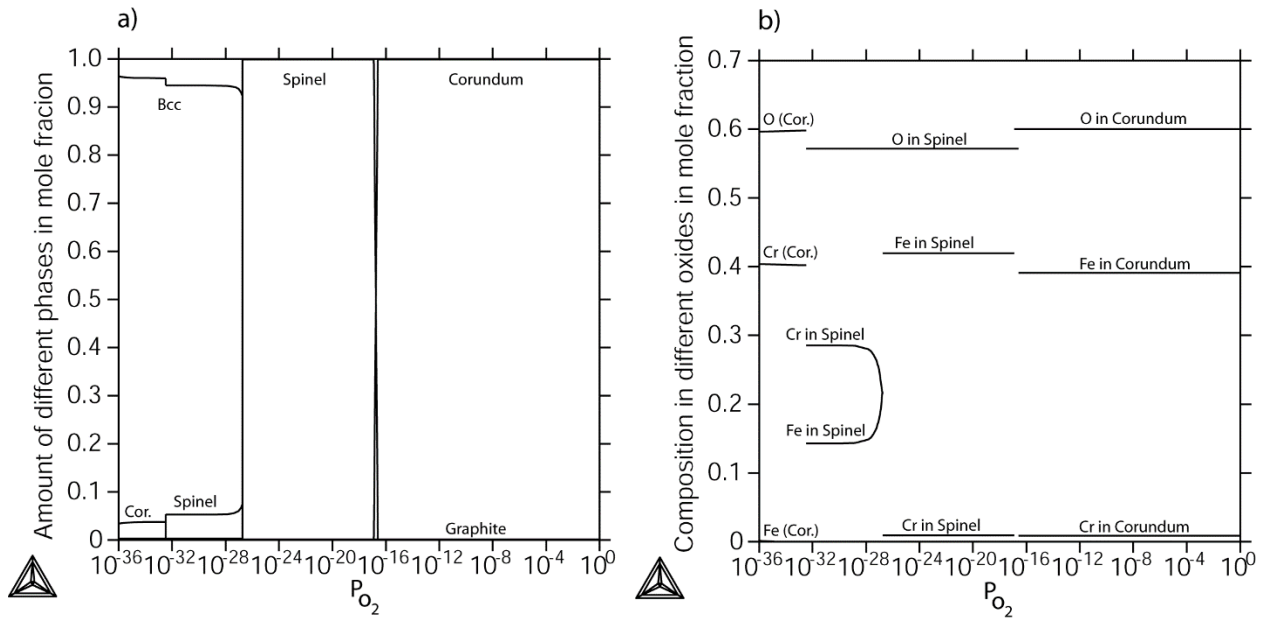


Fig. 2. a) Calculated oxide scale formed on a low-Cr boiler steel (Fe-1.44Cr-0.06C wt.%) at 550 °C. b) Calculated oxygen partial pressure versus composition in different oxides for the same steel as in a. These results agree very well compared with experimental information [17]. A small amount of graphite is present for the whole oxygen partial pressure interval.

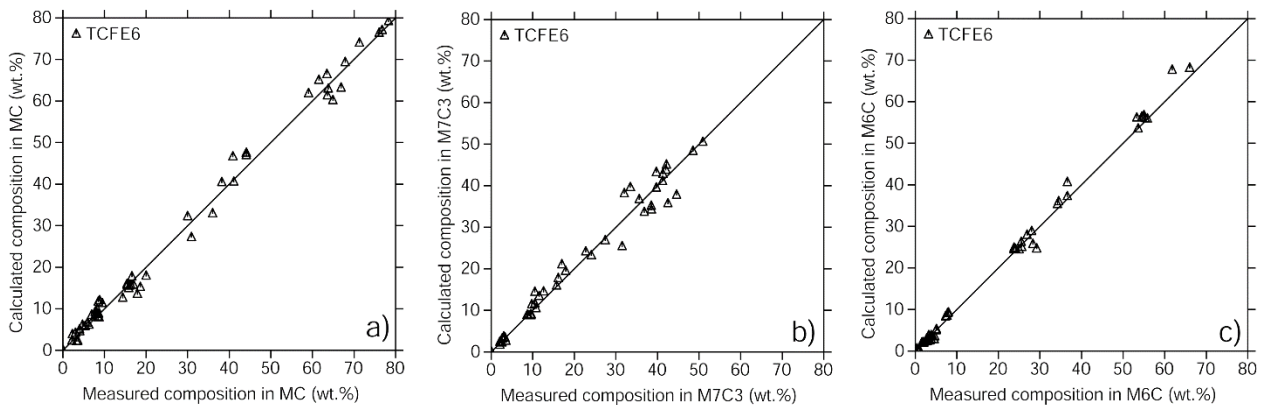


Figure 3. Calculated vs. experimental equilibrium composition for: a) MC, b) M7C3 and c) M6C carbides in different tool steels and high-speed steels. The experimental data has been taken from references 18, 19 and 20.

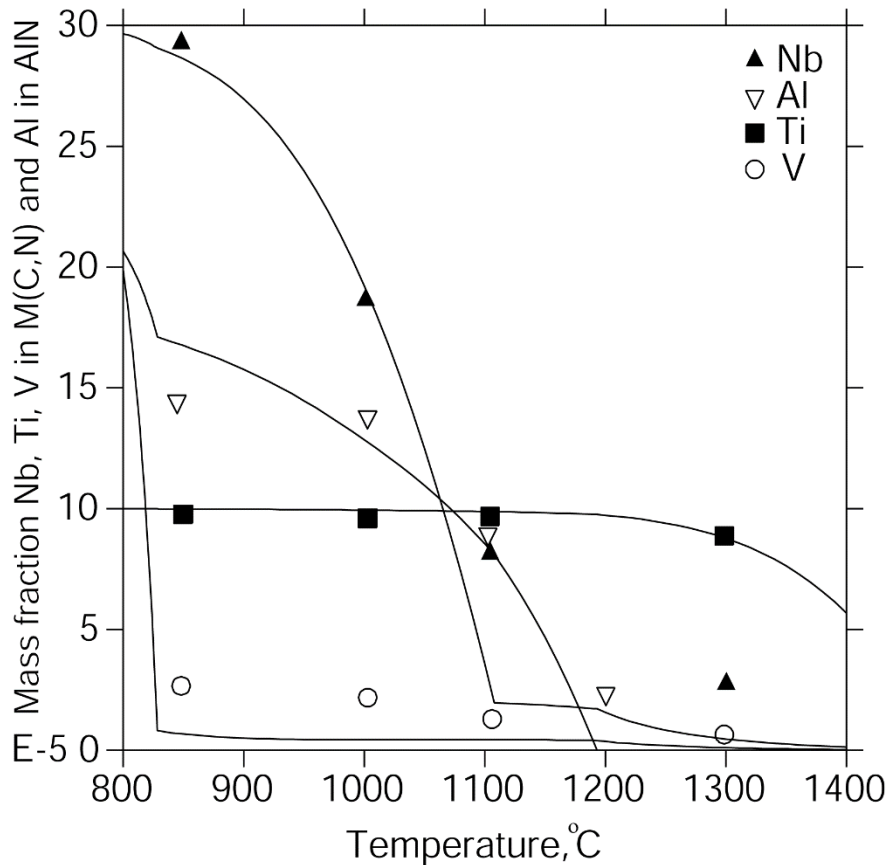


Figure 4. Predicted mass fraction of Nb, Ti, V, and Al in precipitates compared with experimental information[21] for a microalloyed steel with 0.09%C, 1.51%Mn, 0.035%Al, 0.010%Ti, 0.030%Nb, 0.08%V and 0.0105%N (mass percent).

Table 1. Predicted compositions for $(Ti_xNb_{1-x})NyC_{1-y}$ and $(NbtTi_{1-t}Cu_{1-u})$ carbonitrides (site fractions) in two microalloyed steels compared with measurements from Craven et al.[22]. All calculations were made at 1000 °C. Both steels contain the following alloy contents: 0.036%Al, 1.4%Mn, 0.50%Ni, 0.015%P, 0.002%S and 0.4%Si in addition to the composition provided in the table (mass percent).

Steel 1	0.07%C	0.0079%N	0.025%Nb	0.009%Ti
	x	y	t	U
Experiment	0.86 ± 0.04	≈ 1	1	≈ 0.7
Calculation	0.94	0.94	0.98	0.71
Steel 2	0.097%C	0.0049%N	0.017%Nb	0.010%Ti
	x	y	t	U
Experiment	0.91 ± 0.03	0.84 ± 0.05	1 or ≈ 0.8	≈ 1
Calculation	0.97	0.92	0.97	0.78

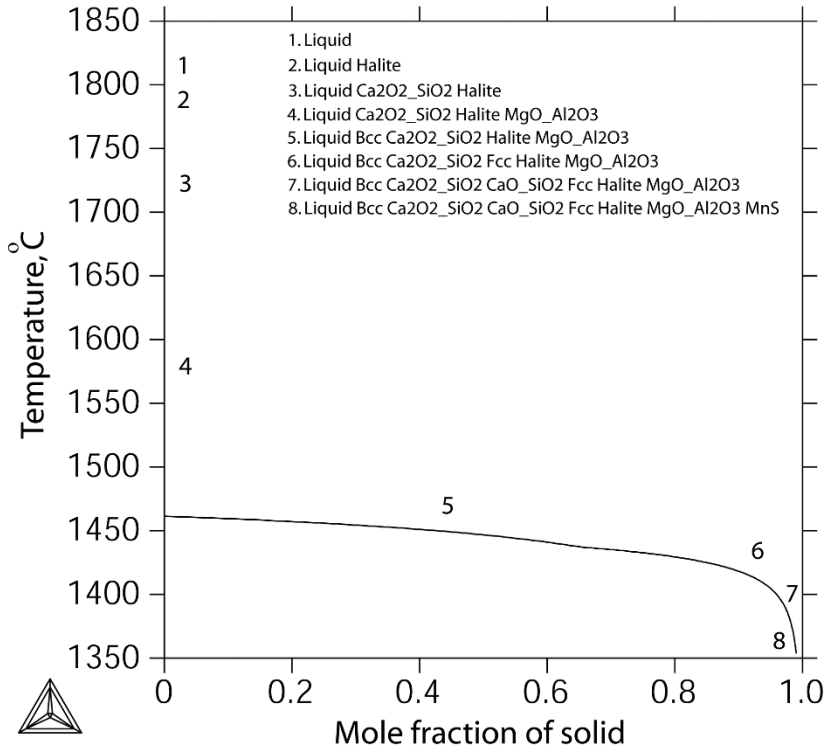


Fig. 5. Scheil simulation for the following alloy in mass percent; Fe-0.02C-0.54Si-0.003Al-0.0005Ca-0.0005Mg-2.19Mo-0.008S-17.01Cr-10.15Ni-0.002O. The Halite phase consists mostly of MgO and the MnS phase is mainly Ca and Mg sulphide. The results fit the experimental data reasonable well[23].

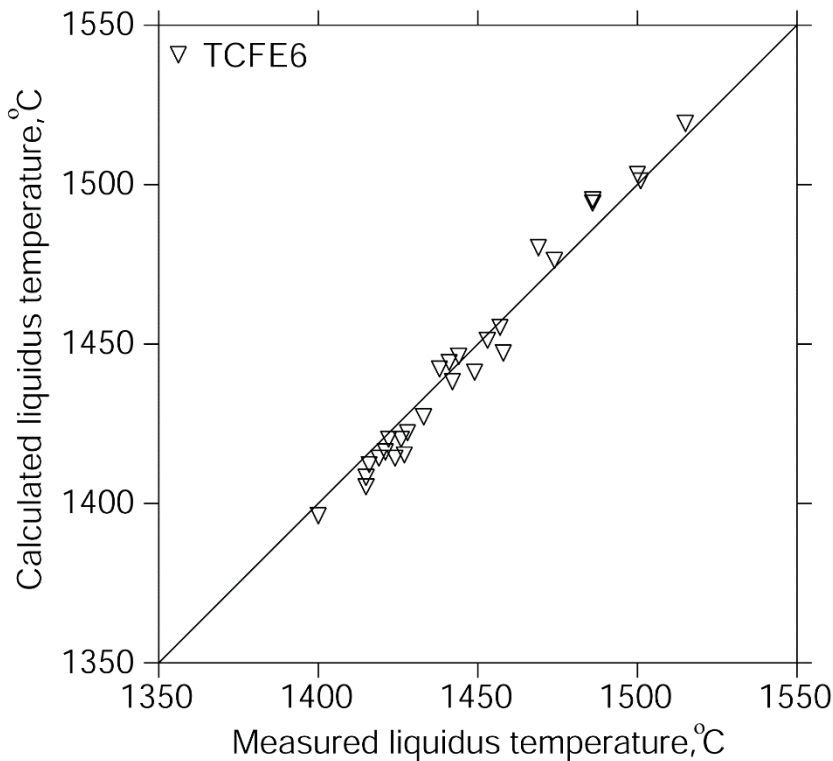


Fig. 6. Experimental liquidus temperatures[24, 25 and 26] for various steels (stainless steels, carbon and low alloy steels, high-speed steels with high Nb content and chromium steels) compared with calculations performed using the TCFE6 databases.

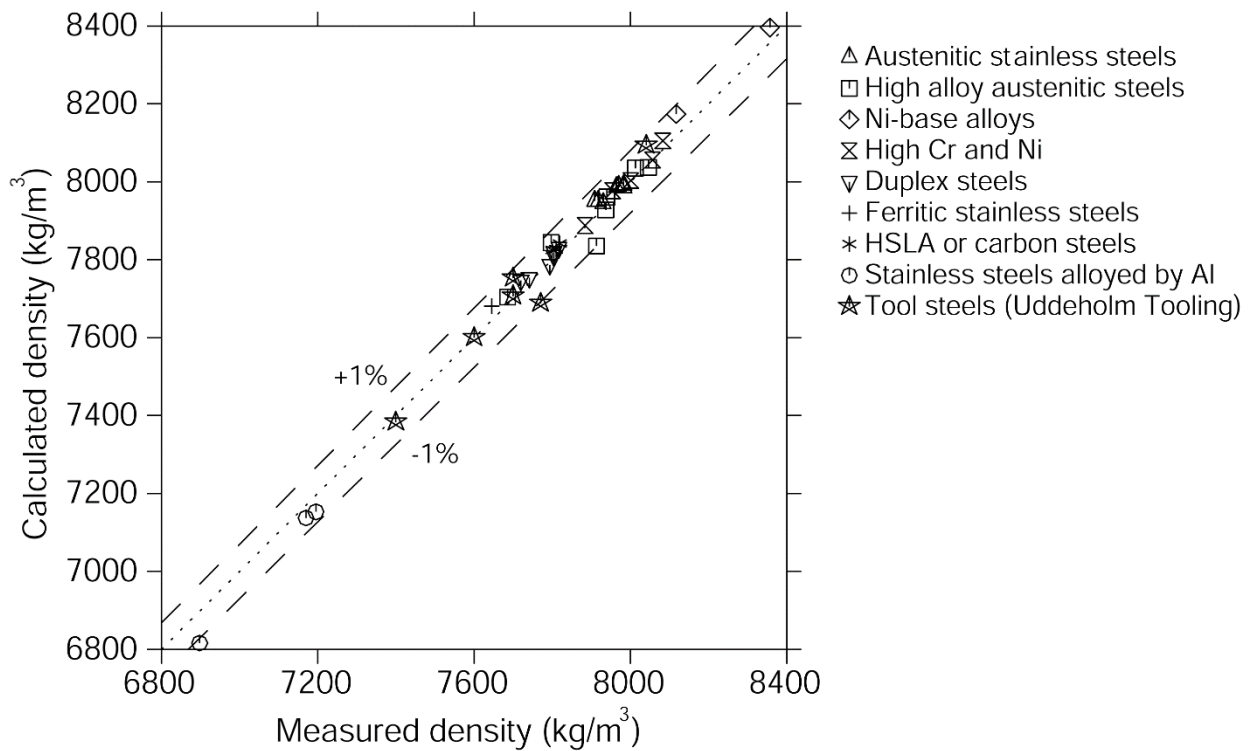


Fig. 7. Calculated density of several different steels at room temperature compared with experimental data provided by Sandvik[27] and Uddeholm Tooling[28].

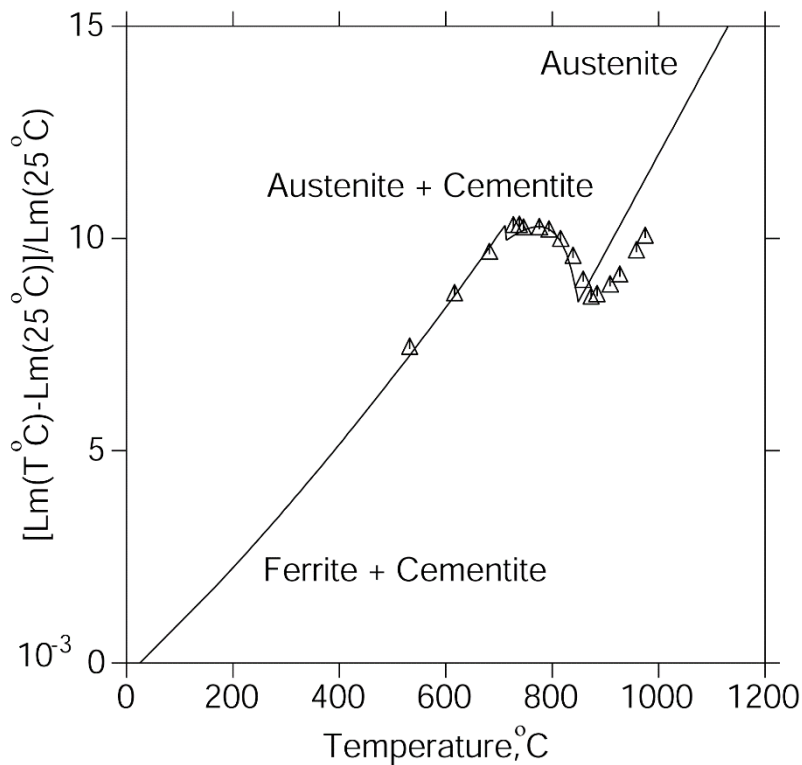


Fig. 8. Relative length change[29] of steel Fe-0.11C-0.5Mn-0.03Si-0.01Cr-0.02Ni (mass percent) compared with predictions using TCFE6.

Acknowledgement

Professor Bo Sundman is acknowledged for many valuable discussions and important contributions. Special acknowledgements are given to associate professor Malin Selleby and doctor Lina Kjellqvist (now at Thermo-Calc Software AB) at the Royal Institute of Technology, Stockholm, Sweden for their contributions in oxide systems[6-11].

References

1. G. Miyamoto, J.C. Oh, K. Hono, T. Furuhashi and T. Maki, *Acta Materialia*, Vol. 55, 2007, pp. 5027-5038.
2. J.-C. Zhao, M.R. Jackson and L.A. Peluso, *Acta Materialia*, Vol. 51, 2003, pp. 6395-6405.
3. J. Fritzsche, G.H. Meier, L. Niewolak, P.J. Ennis, H. Hattendorf, L. Singheiser and W.J. Quadackers, *J. of Power Sources*, Vol. 178, 2008, pp. 163-173.
4. Z. Yang, G.-G. Xia, C.-M. Wang, Z. Nie, J. Templeton, J. Stevenson and P. Singh, *J. of Power Sources*, Vol. 183, 2008, pp. 660-667.
5. European Commission, technical steel research, special and alloy steels, Report EUR 20315, ISBN 92-894-3655-7, 2002.
6. L. Kjellqvist, M. Selleby and B. Sundman, *Calphad*, Vol. 32, 2008, pp. 577-592.
7. L. Kjellqvist and M. Selleby, *Calphad*, Vol. 33, 2009, pp. 393-397.
8. L. Kjellqvist and M. Selleby, Submitted to *J. of Phase Equilibria and Diffusion*, 2009.
9. L. Kjellqvist and M. Selleby, Submitted to *J. of Alloys and Compounds*, 2009.
10. L. Kjellqvist and M. Selleby, Submitted to *International J. of Materials Research*, 2009.
11. L. Kjellqvist, PhD Thesis, KTH Royal Institute of Technology, ISBN 978-91-7415-428-3, Stockholm, Sweden 2009.
12. D. L. Douglas, F. Gesmundo and C. De Asmundis, *Oxidation of Metals*, Vol. 25, 1986, pp. 235-268.
13. D. L. Douglas and F. Rizzo-Assuncao, *Oxidation of Metals*, Vol. 29, 1988, pp. 271-287.
14. P. Nanni, V. Buscaglia, G. Battilana and E. Ruedl, *J. of Nuclear Materials*, Vol. 182, 1991, pp. 118-127.
15. H. Kurokawa, K. Kawamura and T. Maruyama, *Solid State Ionics*, Vol. 168, 2004, pp. 13-21.
16. R. Wang, M. J. Straszheim and R. A. Rapp, *Oxidation of Metals*, Vol. 21, 1984, pp. 71-79.
17. V. B. Trindade, U. Krupp, H.-J. Christ, M. J. Monteiro and F. C. Rizzo, *Mat.-wiss. u. Werkstofftech.*, Vol. 36, No. 10, 2005, pp. 471-476.
18. J. Bratberg and K. Frisk, *Met. Mat. Trans. A*, Vol. 35A, No. 12, 2004, pp. 3649-3663.
19. J. Bratberg and K. Frisk, *Proceeding of the Powder Metallurgy World Congress and EURO-PM2004*, Vienna, Vol. 4, 2004, pp. 337-342.
20. J. Bratberg, *Z. für Metallk.*, Vol. 96, No. 4, 2005, pp. 335-344.
21. S. Zajac, Internal report IM-3566, Swedish Institute for Metals Research, Stockholm, Sweden, 1998.
22. J. Craven, K. He, L. A. J. Garvies and T. N. Baker, *Acta Mater.*, Vol. 48, 2000, pp 3857-3868.
23. O. Ericsson, Personal Communication 2008, Royal Institute of Technology, Stockholm, Sweden.
24. Jernkontoret, "A Guide to the Solidification of Steels", 1977, Stockholm, Sweden.

25. G. Allan, EU technical steel research, Castability, solidification mode and residual ferrite distribution in highly alloyed stainless steels, 1997.
26. G. C. Coelho, J. A. Golczewski and H. F. Fischmeister, Mat. Trans. A, Vol. 34A, No. 9, 2003, pp. 1749-1758.
27. Personal Communication with Sandvik.
28. www.uddeholm.se
29. C. Garcia de Andrés, F. G. Caballero, C. Capdevila and L. F. Álvarez, Materials Characterization, Vol. 48, Issue 1, 2002, pp. 101-111.